Automat Control of the Flight Altitude Using the Dynamic Inversion and the Influence of Wind Shears and Sensors' Errors on the Aircrafts' Landing Process

LUNGU MIHAI
University of Craiova
Faculty of Electrical Engineering, Avionics Division
Blv. Decebal, No.107, Craiova, Dolj
ROMANIA
Lma1312@yahoo.com, mlungu@elth.ucv.ro

MASTORAKIS E. NIKOS
Technical University of Sofia,
Industrial Engineering Department, Sofia,
BULGARIA
mastor@tu-sofia.bg

GRIGORIE T. LUCIAN
University of Craiova
Faculty of Electrical Engineering, Avionics Division
Blv. Decebal, No.107, Craiova, Dolj
ROMANIA
lgrigore@elth.ucv.ro, ltgrigorie@yahoo.com

Abstract: - The paper presents a new system (automat pilot) for the automat control of the aircrafts' flight altitude in the landing process. The system has two subsystems: the first one controls the altitude of the aircrafts in the descendent phase of the landing process, while the second subsystem controls the altitude too, but in the flare phase (the second phase of the landing process). The paper's authors validate the obtained automat pilot by numerical simulations in Matlab neglecting or taking into consideration the wind shears and sensors' errors. They obtained complex Matlab/Simulink models and time characteristics (time variations of the variables involved in the landing process). The wind shears and the sensors' errors don't affect the landing process. The most important graphic characteristic is the dependence between flight altitude and the horizontal displacement.

Key-Words: - Dynamic inversion, Landing process, Sensors' errors, Wind shears

1 Aircrafts' Longitudinal Equations in the Landing Process

For the study of the landing process, the paper's authors obtained the dynamic structure from this paper and the validation of this structure is made by simulations in Matlab medium. First of all, the authors have to present the model of the longitudinal movement for a Charlie-1 aircraft [1].

The main sensors that are used on aircrafts are: three accelerometers (for the measurement of the accelerations a_x, a_y, a_z, which, by integrating, lead to velocities V_x, V_y, V_z) and three gyrometers (for the measurement of the angular velocities $\omega_x, \omega_y, \omega_z$), connected in an inertial navigation system (INS), sensors for static and dynamic pressure (the first for the determination of the barometric altitude and the both sensors for the determination of the flight velocity), a radio-altimeter or other system for the measurement of the aircraft's height with respect to the ground and so on [2], [3].

The state equation that describes the longitudinal movement of the aircraft is

$$\dot{\mathbf{x}} = A\mathbf{x} + Bu, \tag{1}$$

with the state vector $\mathbf{x} = \left[V_x \; V_z \; \omega_y \; \theta\right]^T$, the command vector $u = \left[\delta_p \; \delta_T\right]^T, \delta_T$ – the engine command, δ_p – the deflection of the elevator, θ – the pitch angle, $\omega_y = \dot{\theta}$ – the pitch rate, V_x, V_z – the

components of the velocity vector $\vec{V}$ with respect to the longitudinal axis of the aircraft (Ox axis) and the vertical one (Oz axis), matrices A and B of form

$$A = \begin{bmatrix} a_{11} & a_{12} & a_{13} & a_{14} \\ a_{21} & a_{22} & a_{23} & a_{24} \\ a_{31} & a_{32} & a_{33} & a_{34} \\ a_{41} & a_{42} & a_{43} & a_{44} \end{bmatrix} = \begin{bmatrix} X_u & X_w & 0 & -g\cos\theta_0 \\ Z_u & Z_w & V_0 & -g\sin\theta_0 \\ \widetilde{N}_u & \widetilde{N}_w & \widetilde{N}_q & \widetilde{N}_\theta \\ 0 & 0 & 1 & 0 \end{bmatrix}, \quad (2)$$

$$B = \begin{bmatrix} b_{11} & b_{12} \\ b_{21} & b_{22} \\ b_{31} & b_{32} \\ 0 & 0 \end{bmatrix} = \begin{bmatrix} 0 & X_{\delta_T} \\ Z_{\delta_p} & Z_{\delta_T} \\ \widetilde{N}_{\delta_p} & \widetilde{N}_{\delta_T} \\ 0 & 0 \end{bmatrix};$$

the elements $\widetilde{N}_u, \widetilde{N}_w, \widetilde{N}_q, \widetilde{N}_\theta, \widetilde{N}_{\delta_p}$ are calculated with the formula [4]

$$\begin{aligned} &\widetilde{N}_u = N_u + N_{\dot{w}} Z_u, \widetilde{N}_w = N_w + N_{\dot{w}} Z_w, \\ &\widetilde{N}_q = N_q + N_{\dot{w}} V_{x0}, \widetilde{N}_\theta = -gN_{\dot{w}} \sin\theta_0, \\ &\widetilde{N}_{\delta_p} = N_{\delta_p} + N_{\dot{w}} Z_{\delta_p} \end{aligned} \quad (3)$$

with respect to the stability derivates, which, for an aircraft Charlie-1, have the values [1]

$$\begin{aligned} &X_u = \text{-}0.0238[1/s], X_w = 0.122[1/s], Z_u = -0.2[1/s], \\ &Z_w = -0.512[1/s], N_u = 0.000036[\text{deg}/s \cdot m], \\ &N_w = -0.006[\text{deg}/s \cdot m], N_{\dot{w}} = -0.0008[\text{deg}/m], \\ &X_{\delta_T} = 0.1[m/s/\text{deg}], X_{\delta_T} = -1.69 \cdot 10^{-7}[m/s/\text{deg}], \\ &V_0 = V_{x_0} = 67[m/s], N_{\delta_T} \cong 0, Z_{\delta_p} = -1.96[m/s/\text{deg}], \\ &N_{\delta_p} = 0, \sin\theta_0 \cong 0, \cos\theta_0 \cong 1. \end{aligned} \quad (4)$$

If one chooses the state vector $\mathbf{x} = \begin{bmatrix} V_x & \alpha & \omega_y & \theta \end{bmatrix}^T$, then in matrices A and B the second raw changes

$$\begin{aligned} &Z_u \to Z_u^* = Z_u / V_0, V_0 / V_0 = 1, \\ &-g\sin\theta_0 \to -g\sin\theta_0 / V_0 \cong 0, \\ &b_{21} \to b_{21} / V_0, b_{22} \to b_{22} / V_0. \end{aligned} \quad (5)$$

Thus, the dynamics of the longitudinal movement, for the above mentioned aircraft, is described by the matrices

$$A = \begin{bmatrix} -0.021 & 0.122 & 0 & -9.69 \\ -0.003 & -0.7535 & 0.91 & 0 \\ 0 & -0.245 & -0.213 & 0 \\ 0 & 0 & 1 & 0 \end{bmatrix}, B = \begin{bmatrix} 0 & 0.1 \\ -0.166 & 0 \\ -1.8 & 0 \\ 0 & 0 \end{bmatrix}. \quad (6)$$

For the landing stage, the values of the longitudinal velocity, at the beginning of the descend phase is $V_0 = V_{x_0} = 250[m/s]$, while in the moment when the aircraft begins the flare stage (the second major landing stage, $H = H_0$) it becomes [1]

$$V_a = V_0 - at_a = V_0 = ct. = 67\, m/s. \quad (7)$$

Because $t_a = 32\, s$, the distance R from the aircraft to the intersection point of landing path with the runway is obtained using the formula [1]

$$R = \int_0^t (V_a - at)\,\mathrm{d}t; \quad (8)$$

one yields $R \cong 1806\, m$, while the horizontal covered distance is

$$x_g = R\cos\left(2.5 \cdot \frac{\pi}{180}\right) \cong 1804\, m. \quad (9)$$

The altitude at which the flare maneuver begins is $H_0 \cong 20\, m$. Because one has to impose the value of H_0 (the transition altitude from the landing descendent phase to the flare landing phase), the state vector must contain the variable H (the flight altitude); thus the equations that describe the longitudinal movement of the aircraft in the landing process are [4]

$$\begin{aligned} &\dot{V}_x = X_u V_x + X_w V_z + \widetilde{X}_q \omega_y - g\cos\theta_0 \cdot \theta + X_{\delta_p}\delta_p + X_{\delta_T}\delta_T, \\ &\dot{V}_z = Z_u V_x + Z_w V_z + \widetilde{Z}_q \omega_y - g\sin\theta_0 \cdot \theta + Z_{\delta_p}\delta_p + Z_{\delta_T}\delta_T, \\ &\dot{\omega}_y = \widetilde{N}_u V_x + \widetilde{N}_w V_z + \widetilde{N}_q \omega_y + \widetilde{N}_\theta \theta + N_{\delta_p}\delta_p + N_{\delta_T}\delta_T, \\ &\dot{\theta} = \omega_y, \\ &\dot{H} = V_{x_0}\theta - V_z \Leftrightarrow \dot{H} = V_{x_0}(\theta - \alpha); V_{x_0} = V_0. \end{aligned} \quad (10)$$

In this case, the state equation is again (1), but the state vector becomes

$$\mathbf{x} = \begin{bmatrix} V_x & V_z & \omega_y & \theta & H \end{bmatrix}^T \quad (11)$$

and the matrices A and B get the form

$$A = \begin{bmatrix} a_{11} & a_{12} & a_{13} & a_{14} & 0 \\ a_{21} & a_{22} & a_{23} & a_{24} & 0 \\ a_{31} & a_{32} & a_{33} & a_{34} & 0 \\ 0 & 0 & 1 & 0 & 0 \\ 0 & -1 & 0 & V_0 & 0 \end{bmatrix}, B = \begin{bmatrix} b_{11} & b_{12} \\ b_{21} & b_{22} \\ b_{31} & b_{32} \\ 0 & 0 \\ 0 & 0 \end{bmatrix} \quad (12)$$

or, for the numeric simulation,

$$A = \begin{bmatrix} -0.021 & 0.122 & 0 & -9.69 & 0 \\ -0.003 & -0.7535 & 0.91 & 0 & 0 \\ 0 & -0.245 & -0.213 & 0 & 0 \\ 0 & 0 & 1 & 0 & 0 \\ 0 & -1 & 0 & 67 & 0 \end{bmatrix}, B = \begin{bmatrix} 0 & 0.1 \\ -0.166 & 0 \\ -1.8 & 0 \\ 0 & 0 \\ 0 & 0 \end{bmatrix}. \quad (13)$$

2 Inversion of the Aircrafts' Dynamic Model

Flight automat control structures are based on the dynamic inversion principle [5]. Thus, the linear dynamic model of the aircraft's rotation movement is described by equation

$$\dot{\omega} = A_\omega \omega + A_v V + B\delta_c , \quad (14)$$

with $\omega = \begin{bmatrix} \omega_x & \omega_y & \omega_z \end{bmatrix}^T$ – the vector containing the angular velocities of the aircraft, $V = \begin{bmatrix} V_x & V_y & V_z \end{bmatrix}^T$ – the aircraft's translations velocities vector (with its components), $\delta_c = \begin{bmatrix} \delta_p & \delta_e & \delta_d \end{bmatrix}^T$ – the vector containing the command deflection of the elevator (δ_p), the command deflection of the ailerons (δ_e) and the command deflection of the rudder (δ_d); A_ω and A_v – (3×3) matrices that define the rotations and the translations of the aircraft, $B - (3\times 3)$ inversable input matrix. By dynamic inversion, the control law

$$\delta_c = B^{-1}\left(\dot{\omega} - A_\omega \omega - A_v V\right) \quad (15)$$

is obtained.

The authors also use the first differential equation extracted from state equation (1), where $a_{13} = b_{11} = 0$; the two equations are

$$\dot{\omega}_y = a_{31}V_x + a_{32}V_z + a_{33}\omega_y + b_{21}\delta_p , \quad (16)$$

$$\dot{V}_x = a_{11}V_x + a_{12}V_z + a_{14}\theta + b_{12}\delta_T . \quad (17)$$

It results the equations of the inversed model for the aircraft longitudinal movement

$$\delta_p = \frac{1}{b_{21}}\left(\dot{\omega}_{y_c} - a_{31}V_x - a_{32}V_z - a_{33}\omega_y\right), \quad (18)$$

$$\delta_T = \frac{1}{b_{12}}\left(\dot{V}_{x_c} - a_{11}V_x - a_{12}V_z - a_{14}\theta\right). \quad (19)$$

For the obtaining of the command inputs of the aircrafts flight' automat control subsystems, one uses a reference model (command filter – low pass filter). The subsystem's order, represented by each command filter, is equal with the relative degree of the subsystem's model whose output is the state variable commanded by the respective filter's output. Thus, for the command of the pitch angle (θ), one uses a filter with the transfer function

$$\frac{\overline{\theta}(s)}{\theta_c(s)} = \frac{\omega_n^2}{s^2 + 2\xi\omega_n s + \omega_n^2}, \quad (20)$$

with ω_n – the frequency (natural pulsation) and ξ – the damping coefficient. The filter provides the output signals $\overline{\theta}, \dot{\overline{\theta}}, \ddot{\overline{\theta}}$ and, by the integration of $\overline{\theta}$, $\int \overline{\theta}\, dt$ may also be obtained. With these signals the components of the angular acceleration $\ddot{\theta}_c$ may be calculated [6]

$$\ddot{\theta}_c = \dddot{\overline{\theta}} + k_p^{\theta}\left(\ddot{\overline{\theta}} - \ddot{\theta}\right) + k_p^{\dot{\theta}}\left(\dot{\overline{\theta}} - \dot{\theta}\right) + k_{pi}^{\theta}\int\left(\overline{\theta} - \theta\right)dt . \quad (21)$$

For the obtaining of imposed angular accelerations, the authors uses a PID controller (proportional – integral – derivative controller) [7], [8]; the derivative component stabilizes the system with angular velocity steady error equal with zero, the integral component assures the zero steady errors for all the angular variables while the angular acceleration $\dddot{\overline{\theta}}$ leads to faster time responses.

The expression of the imposed angular acceleration $\dot{\overline{\omega}}_y$ is obtained by the derivation of the equation [4]

$$\omega_y = \dot{\theta}\cos\varphi + \dot{\psi}\cos\theta\sin\varphi , \quad (22)$$

where $\dot{\omega}_y$ and $\ddot{\theta}$ are replaced by $\dot{\overline{\omega}}_y$ and $\ddot{\theta}_c$; it yields

$$\dot{\omega}_{y_c} = \ddot{\theta}_c\cos\varphi - \dot{\theta}\dot{\varphi}\sin\varphi + \ddot{\psi}_c\cos\theta\sin\varphi + \\ + \dot{\psi}\left(\dot{\varphi}\cos\theta\cos\varphi - \dot{\theta}\sin\theta\sin\varphi\right). \quad (23)$$

Angular velocity $\ddot{\theta}_c$ from equation (23) is obtained using equation (21). For the longitudinal movement

$$\dot{\omega}_{y_c} = \ddot{\theta}_c . \quad (24)$$

The velocity V_x is controlled by the mean of the motor command δ_T using equation (19). The aircraft's speed must be constant during the landing process to prevent landing accidents. Taking into account that the relative degree of the aircraft dynamic model with respect to the state variable is 1, the reference model (command filter) must be chosen with the transfer function

$$\frac{\overline{V}_x(s)}{\overline{V}_{x_c}(s)} = \frac{1}{T_x s + 1}. \quad (25)$$

Because of the slow dynamics of the engine, T_x has large value; for example $T_x = 10^3\, s$. The reference model provides signals that are function of $\overline{V}_x$ and $\dot{\overline{V}}_x$. The imposed acceleration is formed using the signal [9]

$$\dot{V}_{x_c} = \dot{\overline{V}}_x + k_x\left(\overline{V}_x - V_x\right) + k_{xi}\int\left(\overline{V}_x - V_x\right)dt + \\ + k_d s\left(\overline{V}_x - V_x\right). \quad (26)$$

Thus, the chosen controller is a PID one. For the longitudinal movement model (13), the authors chooses the values

$$k_x = 20\, s^{-1}, k_{xi} = 0.01 s, k_d = 1.4 . \quad (27)$$

At the input of the command filter one applies the signal V_{x_c} (in fact a variation of the velocity V_x); for example, one chooses $\overline{V}_{x_c} = 10m/s$. The time constant is $T_T = 5s$. The subsystem for the control of the velocity is a part of the system from fig.1 (automat control system of the aircraft flight in longitudinal plane).

3 Description of the Automat Control of the Flight Altitude Based on Dynamic Inversion

For the control of the flight altitude H, an exterior loop and an interior loop (for the control of the pitch angle - fig.1) are used. The controller for θ is a PID one – equation (21) with the coefficients

$$\begin{aligned} k_p^\theta &= 50\left[(\text{deg}/s^2)/\text{deg}\right], \\ k_p^{\dot\theta} &= 10\left[(\text{deg}/s^2)/(\text{deg}/s)\right], \\ k_{pi}^\theta &= 2\left[(\text{deg}/s^2)/(\text{deg}\cdot s)\right]. \end{aligned} \quad (28)$$

The inverse model is described by equation (18) and the command filter has the form (20), with $\omega_n = 3rad/s$ and $\xi = 0.7$.

For the altitude's control, the authors use a PI controller, but, to control the descending velocity $\dot H$ too, they choose a PID controller described by equation [10]

$$\theta_c = k_p^h(H_c - H) + k_{pi}^h\int(H_c - H)\,\mathrm{d}t + k_p^{\dot h}\dot H_c, \quad (29)$$

where the desired (calculated) descendent velocity is expressed with the formula

$$\dot H_c = V_{x_c}\gamma_c; \quad (30)$$

γ_c is the imposed (calculated) value of the landing trajectory path; one chooses $\gamma_c = -2.5\,\text{deg}$. For the model (13), the following values have been chosen

$$k_p^h = 0.5\,[\text{deg}/m],\ k_{pi}^h = 10^{-4}\,[\text{deg}/m\cdot s],\ k_p^{\dot h} = 0.02. \quad (31)$$

For the calculus of H_c, for the first phase of the landing process $(H \ge H_0)$, one uses equation

$$H_c = (x - x_{p_0})\cdot\tan(\gamma_c),\ H \ge H_0. \quad (32)$$

For an instantaneous point $A_p(x_p, H_p)$, the above equation is equivalent with the following one

$$x_{p_0} = x_p - H_p/\tan(\gamma_c). \quad (33)$$

So, for the descend phase of the landing process, the equation (32) is used, with x_{p_0} of form (33) and with $\gamma_c = -2.5\,\text{deg}$. For the flare process $(H < H_0)$, the expression of H_c is

$$H_c = H_0\cdot\exp\left(-\frac{t-t_0}{\tau}\right),\ H_0 = H(t_0), \quad (34)$$

t_0 being the moment when the aircraft passes from the descend phase to the flare stage. Taking into account that

$$t - t_0 = \frac{x - x_0}{\dot x}, \quad (35)$$

the equation (34) becomes

$$H_c = H_0\cdot\exp\left(-\frac{x-x_0}{\tau\cdot\dot x}\right),\ H < H_0. \quad (36)$$

For the studied example, $\tau = 8\,s$ and $T_p = 0.1\,s$.

The horizontal displacement velocity is calculated with

$$\dot x = V_x\cos\theta + V_z\sin\theta. \quad (37)$$

In fig.1 the authors present the aircrafts' automat control system for the landing process in the longitudinal plane.

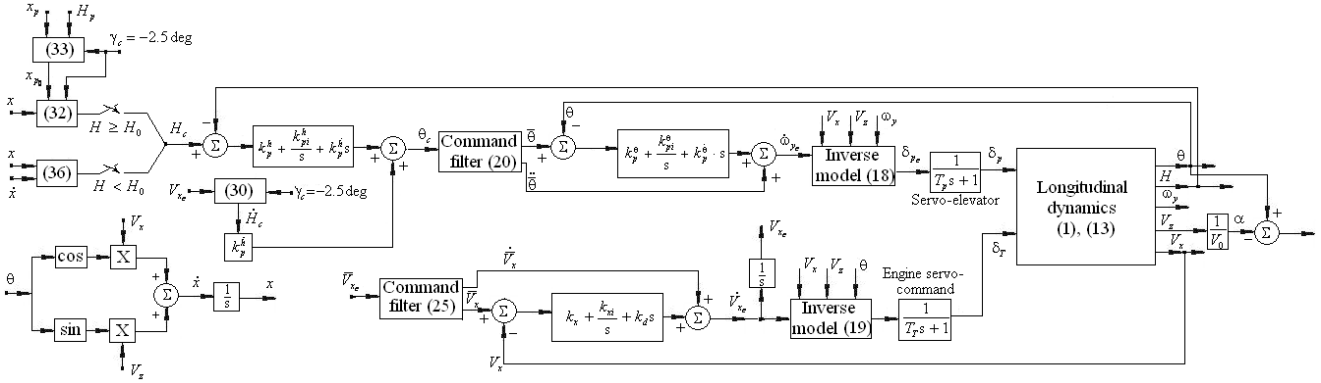

Fig.1 Aircrafts' automat control system for the landing process in the longitudinal plane

4 Computer Simulations

If the wind shears are taken into consideration, the aircraft dynamics change. The linear model of the aircraft's movement, in longitudinal plane, becomes

$$\dot{\mathbf{x}} = A\mathbf{x} + Bu + B_v v_v \,, \tag{38}$$

with $\mathbf{x}$ - the state vector, u – the command vector, v_v – the disturbances' vector (the components of the wind velocity on aircraft axes Ox and Oz),

$$\mathbf{x} = \left[V_x \;\; \alpha \;\; \omega_y \;\; \theta\right]^T, u = \left[\delta_p \;\; \delta_T\right]^T, v_v = \left[V_{vx} \;\; V_{vz}\right]^T, \tag{39}$$

$$B_v = \begin{bmatrix} -a_{11} & -a_{21} & -a_{31} & 0 \\ -a'_{12} & -a'_{22} & -a'_{32} & 0 \end{bmatrix}^T; \tag{40}$$

$$B_v = \begin{bmatrix} -a_{11} & -a_{21} & -a_{31} & 0 \\ -a_{12}/57.3V_0 & -a_{22}/57.3V_0 & -a_{32}/57.3V_0 & 0 \end{bmatrix}^T;$$

the elements of the matrix B_v are calculated with the equations from [4], with respect to the stability derivates for the aircraft's type.

The calculus equations for the components of the wind's velocity may be of forms [11], [12]

$$V_{vx} = -V_{vx_0}\sin(\omega_0 t), V_{vz} = -V_{vz_0}\left[1-\cos(\omega_0 t)\right], \quad \omega_0 = 2\pi / T_0 \,. \tag{41}$$

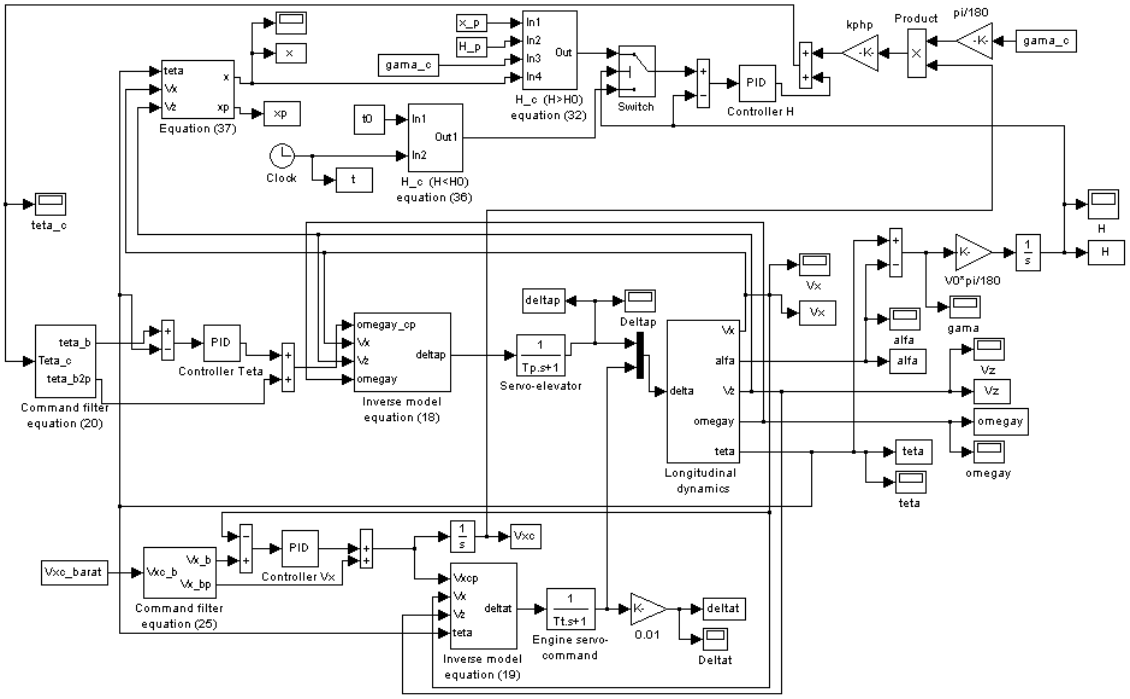

Fig.2 The Matlab/Simulink model for the block diagram from fig.1.

By the simulation of the Matlab/Simulink model from fig.2, the authors obtained the time characteristics from fig.3, fig.4 and fig.5. In fig.3 the authors presented the time variations of α, γ, ω_y, V_x, V_z, $\theta, \delta_p, \delta_T$ and H for the first phase of the landing process – the descendent phase. The characteristics with blue solid line correspond to the case when the landing process isn't affected by the wind shears (the wind velocity is neglected). The characteristics with red dashed line correspond to the landing process affected by wind shears. Same characteristics, but for the second phase of the landing process – the flare phase, are presented in fig.4.

In fig.5 one presents the variation of the altitude H with respect to the horizontal displacement x for the whole landing process (blue solid line for the case "without wind" and red dashed line for the case "with wind"). As one can see, the variation of altitude in the descendent phase is linear, while, in the flare phase, the altitude descends aperiodically and tends to zero. Time variations of the altitude can also be seen in the last graphic from fig.3 (descendent phase) and fig.4 (flare phase).

The wind with the components (41) doesn't disturb the landing process. Thus, the automat pilot from fig.1 is a robust one, with good results.

For the obtaining of the graphics from fig.3 and fig.4, the Matlab/Simulink model from fig.2 has been used. Because the landing process has two important phases, the system from fig.1 has 2 important subsystems: the system for the automat control of the flight altitude in the descendent phase and the system for the automat control of the flight altitude in the flare phase.

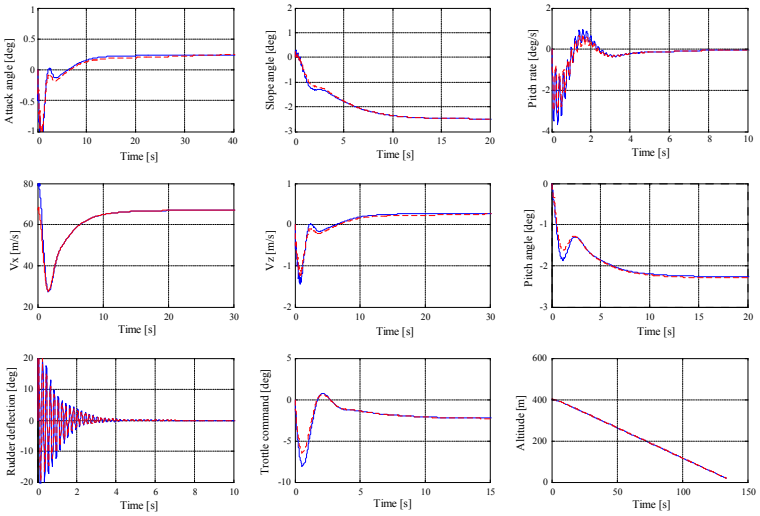

Fig.3 Time variations of the landing process's variables in the first phase – descendent phase

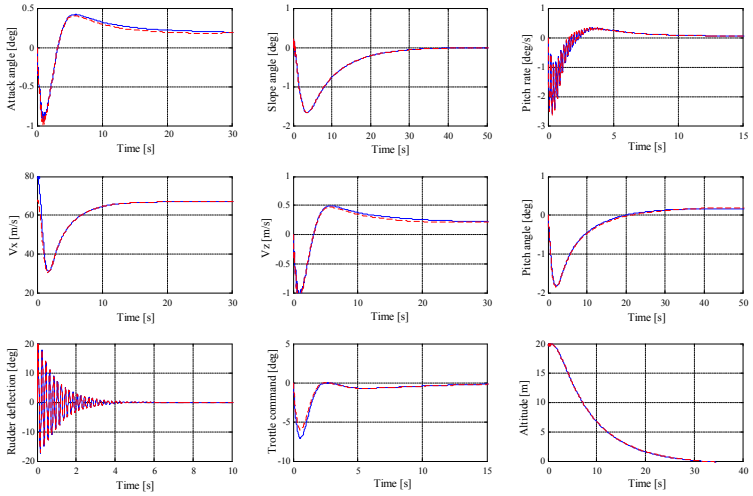

Fig.4 Time variations of the landing process's variables in the second phase – flare phase

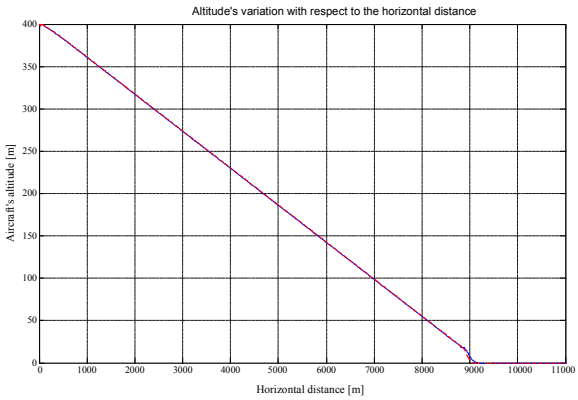

Fig.5 The time variation of the flight altitude for the entire landing process

The graphics from fig.3 have been obtained using the first subsystem, while graphics from fig.4 have been obtained using the second subsystem.

In the above simulations one didn't take into consideration the errors of the sensors (used for the state variables' measurement). These errors are considered in simulations below.

For the determination of the pitch angle θ one may use an integrator gyro. This gyro has errors and it is interesting to see if the sensor's errors affect the landing process. One considers the error's model that takes into account the parameters from the data sheets offered by the sensors' producers; the error's model is described by the equation

ISBN: 978-1-61804-011-4

$$\theta = (\theta_i + S \cdot a_r + B + \nu)\left(1 + \frac{\Delta K}{K}\right), \qquad (42)$$

where θ is the output pitch angle (the perturbed signal), θ_i – the input pitch angle, S – the sensibility to the acceleration a_r applied on an arbitrary direction, B – the bias, K – the scale factor, ΔK – the calibration error of the scale factor and ν – the sensor's noise.

A Matlab/Simulink model has been introduced in the model from fig.2 in the feedback after the pitch

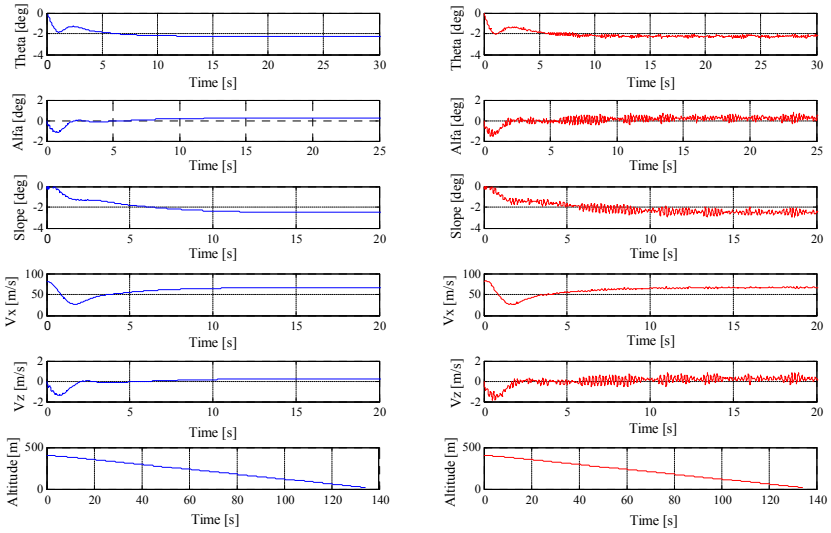

Fig.6 The influence of sensor' errors in the descendent phase of the landing process

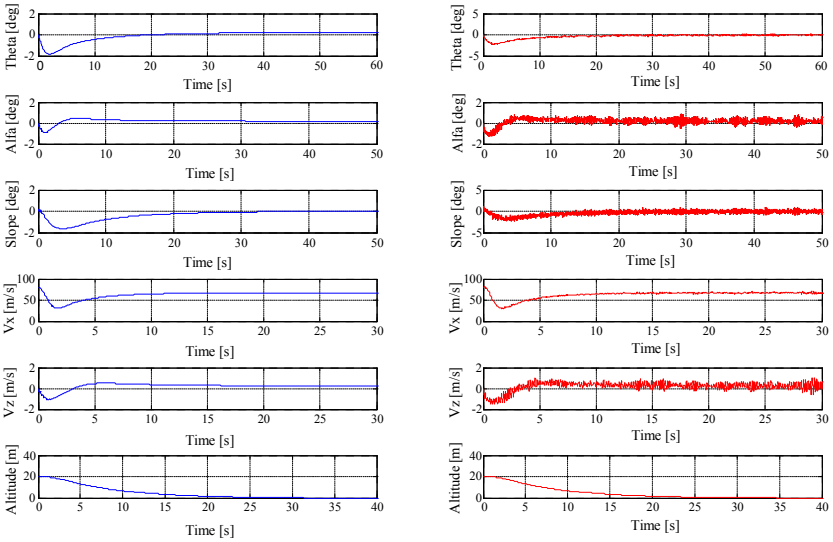

Fig.7 The influence of sensor' errors in the flare phase of the landing process

angle θ. The bias is given by its maximum value B as percentage of span, the calibration error of the scale factor is given by its absolute maximum value ΔK as percentage of K, while the noise is given using its maximum density's value. Using the Matlab function "rand(1)" one generates the bias, by a random value in the interval $(-B, B)$, the sensibility S to acceleration a_r, applied on an arbitrary direction in the interval $(0, S)$ and the calibration error of the scale factor in the interval $(-\Delta K, \Delta K)$. The noise is generated by the mean of a Simulink block "Band-Limited White Noise" using the Matlab function "RandSeed" generating a random value of its density in the interval $(80\% \cdot \nu_d, \nu_d)$.

The error model's inputs are the pitch angle θ_i, and the acceleration a_r, considered to be the resultant acceleration signal that acts upon the carry vehicle, while the output is the disturbed pitch angle θ. In the numerical simulation, the following sensors' parameters have been used: the noise's density - $0.1\left[\text{deg}/\sqrt{Hz}\right]$, the bias - $5\left[\text{deg}\right]$, the error

of the scale factor - $1\% \cdot K$, the sensibility to accelerations - $0.18[\text{deg}/g]$; $\vec{g}$ is the gravitation acceleration.

Although the errors of the gyro sensor (for the measurement of the pitch angle) affect most of the variables, the time variation of the altitude and the time length of the landing process's phases are not affected. So, the authors conclude that the sensor's errors don't affect the landing process.

5 Conclusion

The new system (automat pilot) presented in this paper may be used, with good results, to the automat control of the aircrafts' flight altitude in the landing process. The system has two subsystems: the first one controls the altitude of the aircrafts in the descendent phase of the landing process, while the second subsystem controls the altitude too, but in the second phase of the landing process (flare phase).

The paper's authors validate the obtained automat pilot by numerical simulations in Matlab/Simulink; they obtained a lot of time characteristics (time variations of the variables involved in the landing process) in the presence or in the absence of wind shears. The wind with the components (41) doesn't disturb the landing process, the automat pilot from fig.1 being a robust one.

Interesting results have also been obtained taking into account the sensors' errors (the bias, the scale factor, the calibration error of the scale factor and the sensor's noise). Although the errors of the gyros sensor (for the measurement of the pitch angle) affect most of the variables, the time variation of the altitude and the time length of the landing process's phases are not affected. So, the authors conclude that the sensor's errors don't affect the landing process.

The variation of altitude in the descendent phase is linear, while, in the flare phase, the altitude descends aperiodically and tends to zero. The authors intend in the future to project an automat pilot, based on dynamic inversion too, for the lateral movement of the aircrafts.

Acknowledgment

This work was supported by CNCSIS-UEFISCSU, project PN II-RU "High-precision strap-down inertial navigators, based on the connection and adaptive integration of the nano and micro inertial sensors in low cost networks, with a high degree of redundance", code102/2010.

References:

[1] Mc.L. Donald, *Automatic Flight Control Systems.* Prentice Hall Publisher, 1990, 593 pp.

[2] V. Ricny, J. Mikulec, "Measuring flying object velocity with CCD sensors". *IEEE Aerospace and Electronic Systems Magazine*, vol.9, Issue 6, pp. 3-6, June 1994.

[3] B. Gollomp, The angle of attack. *IEEE Instrumentation & Measurement Magazine*, vol.4, Issue 1, pp. 57-58, 2001.

[4] M. Lungu, *Sisteme de conducere a zborului.* Sitech Publisher, 2008.

[5] Mackunis, P.M. Patre, M.K. Kaise, W.E. Dixon, Asymptotic Tracking for Aircraft via Robust and Adaptive Dynamic Inversion Methods, *IEEE Transactions on Control Systems and Technology*, vol. 18, no.6, 2010.

[6] A.J. Calise, R.T. Rysdyk, Adaptive Model Inversion Flight Control for Tiltrotor Aircraft, *AIAA Guidance, Navigation and Control,* vol. 22, pp. 402-407, 1999.

[7] C. Huang, Q. Shao, P. Jin, Z. Zhu, P. Luoyang, Pitch Attitude Controller Design and Simulation for a Small Unmanned Aerial Vehicle. International Conference on Intelligent Human-Machine Systems and Cybernetics, IHMSC '09, Hangzhou, Zhejiang, 26-27 Aug. 2009, pp. 58-61.

[8] S. Santos, N. Oliveira, Test platform to pitch angle using hardware in loop. 39th IEEE Frontiers in Education Conference, FIE '09, San Antonio, 18-21 Oct. 2009, pp. 1-5.

[9] V. Kargin, *Design of An Autonomous Landing Control Algorithm for A Fixed Wing UAV*. MS Thesys, Middle East Technical University, Ankara, Turkey, 2007.

[10] A.A. Pashilkar, N. Sundararajan, P.A. Saratchandran, Fault-Tolerant Neural Aided Controller for Aircraft Auto-Landing. *Aerospace Science and Technology,* vol.10, Issue 1. 2006, pp. 49-61.

[11] J. Che, D. Chen, Automatic Control using H_∞ Control and Stable Inversion. Proceedings of the 40th IEEE Conference on Decision and Control, Orlando, Florida, USA, 2011, pp. 241–246.

[12] W. Kang, A. Idiori, Flight Control in a Wind shear via Nonlinear H_∞ Methods. Proceedings of the 31th Conference on Decision and Control, Orlando, Florida, USA, 2011, pp. 1135–1142.